Inorganic Chemistry
Article
pubs.acs.org/IC

Fe–TPP Coordination Network with Metalloporphyrinic Neutral Radicals and *Face-to-Face* and *Edge-to-Face* π–π Stacking

Arkaitz Fidalgo-Marijuan,[†] Gotzone Barandika,*[,‡] Begoña Bazán,[†] Miren Karmele Urtiaga,[†] Luis Lezama,[§] and María Isabel Arriortua[†]

[†]Departamento de Mineralogía y Petrología and [§]Departamento de Química Inorgánica, Facultad de Ciencia y Tecnología, Universidad del País Vasco (UPV/EHU), Apartado 644, 48080 Bilbao, Spain

[‡]Departamento de Química Inorgánica, Facultad de Farmacia, Universidad del País Vasco (UPV/EHU), Paseo de la Universidad 7, 01006 Vitoria-Gasteiz, Spain

Supporting Information

ABSTRACT: Compound ([FeTPPbipy]$^\bullet$)$_n$ (TPP = *meso*-tetraphenylporphyrin and bipy = 4,4′-bipyridine) is the first example of a Fe–TPP–bipy coordination network, and it consists of 1D polymers packed through *face-to-face* and *edge-to-face* π–π interactions. The compound has been investigated by means of X-ray diffraction, IR, Mössbauer, UV–visible, and EPR spectroscopies, thermogravimetry, magnetic susceptibility measurements, and quantum-mechanical density functional theory (DFT) and time-dependent DFT calculations. The chemical formula for this compound can be confusing because it is compatible with Fe^{II} and TPP^{2-} anions. However, the spectroscopic and magnetic properties of this compound are consistent with the presence of low-spin Fe^{III} ions and [FeTPPbipy]$^\bullet$ neutral radicals. These radicals are proposed to be formed by the reduction of metalloporphyrin, and the quantum-mechanical calculations are consistent with the fact that the acquired electrons are located on the phenyl groups of TPP.

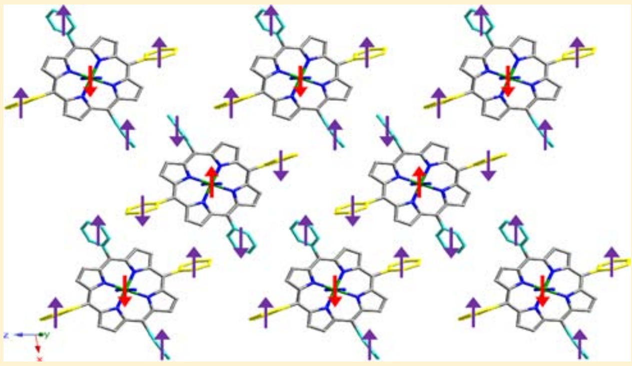

■ INTRODUCTION

Metalloporphyrins are one of the cornerstones on which the existence of life is based because major biochemical, enzymatic, and photochemical functions depend on the special properties of the tetrapyrrolic macrocycle.[1] Thus, porphyrin catalysts are well-known to be highly efficient for oxidative reactions,[2] and during the last years, great effort has been devoted to the immobilization of distinct types of catalysts on solid surfaces,[3−5] with porphyrins also having been investigated in this field.[6−16] Thus, these compounds can also be used for coordination networks where the assembly of metalloporphyrinic structural units can be achieved by coordination bonds and other weaker cohesion forces.[17,18] There are many examples of metalloporphyrinic three-dimensional (3D) frameworks, but most of them consist of the crystallization of monomeric complexes, with the cohesion forces being hydrogen bonds and π stacking. In fact, if thinking of high dimensionality in terms of the formation of coordination polymers, metalloporphyrins exhibit important limitations. To illustrate this point, the case of *meso*-tetraphenylporphyrin (TPP) can be cited. CSD research indicates the existence of monomers, dimers, trimers, and other types of aggregates. However, the highest dimensionality achieved with pyridyl ligands connected on axial positions for octahedral specimens corresponds to one-dimensional (1D) coordination polymers, and just seven of them have been prepared so far.[19−24] It is also worth mentioning that none of them has iron (Fe) as the metal center. In fact, as far as we are aware, the highest dimensionality found for Fe–TPP–dipyridyl systems consists of dimers. However, it must be pointed out that there are two previous examples in the literature for 1D Fe–TPP polymers with cyanide-based ligands.[25,26]

The work herein presented was inspired by previously reported metalloporphyrinic frameworks exhibiting bipyridyl ligands.[27−34] Our intention was the synthesis of high-dimensional frameworks in which metalloporphyrins play two roles: as building blocks in porous networks and as catalysts immobilized in the pores. We still have not achieved this goal, but instead we have synthesized and characterized the compound ([FeTPPbipy]$^\bullet$)$_n$, where bipy is 4,4′-bipyridine (bipy). The compound exhibits 1D coordination polymers that crystallize in a 3D framework in which both *face-to-face* and *edge-to-face* π stacking of the phenyl groups provide stability to the lattice. The main interest of this compound lies in the fact that it is the first Fe–TPP–bipy compound characterized so far. Additionally, the special characteristics of this compound have produced an intricate discussion based on an exhaustive characterization [X-ray diffraction, IR, Mössbauer, UV–visible, and EPR spectroscopies, thermogravimetry, magnetic susceptibility measurements, and quantum-mechanical

Received: March 26, 2013
Published: June 25, 2013

density functional theory (DFT) and time-dependent DFT (TD-DFT) calculations].

■ EXPERIMENTAL SECTION

Materials. All solvents and chemicals were used as received from reliable commercial sources. The reagents 5,10,15,20-tetraphenylporphinyliron(III) chloride (FeTPP-Cl) and 4,4′-bipyridine (bipy; 98%) and the solvent *N*,*N*-dimethylformamide (DMF; 99.8%) were purchased from Sigma-Aldrich Co.; absolute ethanol was purchased from Panreac.

Physicochemical Characterization Techniques. The IR spectrum was collected on a JASCO FT/IR-6100 spectrometer at room temperature in the range of 4000−400 cm^{-1} in KBr pellets (1% of the sample). C, H, and N elemental analyses were measured using a Euro EA 3000 elemental analyzer. UV−visible diffuse-reflectance measurements were carried out on a Cary 5000 UV−visible−near-IR spectrophotometer in the range of 200−2500 nm. Thermogravimetric analyses were carried out using a NETZSCH STA 449F3 thermobalance. A crucible containing 10 mg of sample was heated at 5 °C min^{-1} in the temperature range of 30−500 °C. Mössbauer spectra were obtained at room temperature using a constant-acceleration Mössbauer spectrometer with a $^{57}Co/Rh$ source. The velocity calibration was done using a metallic Fe foil. Electron paramagnetic resonance (EPR) spectra were measured with a Bruker ESP-300 spectrometer operating at X band and equipped with a nitrogen and helium cryostat. Magnetic susceptibility measurements were measured in the range of 4−300 K with a Quantum Design SQUID MPMS-7T magnetometer.

X-ray Structure Determination. Prismatic dark-blue single crystals of $([FeTPPbipy]^{\bullet})_n$ with dimensions given in Table 1 were selected under a polarizing microscope and mounted on MicroMounts. Single-crystal X-ray diffraction data were collected at 100 K on an Xcalibur 2 automatic diffractometer with graphite-monochromated Mo Kα radiation (λ = 0.71073 Å). The Lorentz polarization and absorption corrections were made with the diffractometer software, taking into account the size and shape of the crystals.[35] The structure was solved in the monoclinic space group *C*2/*c* by direct methods with the *SHELXS-97* program.[36] Refinement of the crystal structure was performed by full-matrix least squares based on F^2, using the *SHELXL-97* program.[36] Anisotropic thermal parameters were used for all non-H atoms (Figure S1, Supporting Information). All H atoms connected to the aromatic rings (C−H 0.95 Å) were fixed geometrically and were refined using a riding model with common isotropic displacements. Brief crystal data are listed in Table 1. (See Tables S1−S4, Supporting Information, for bond distances and angles, atomic coordinates, and anisotropic displacement.)

Table 1. Crystallographic Data for $([FeTPPbipy]^{\bullet})_n$

compound	$([FeTPPbipy]^{\bullet})_n$
formula	$C_{54}H_{36}FeN_6$
fw, g mol^{-1}	824.74
cryst syst	monoclinic
space group	*C*2/*c* (No. 15)
a, Å	21.6833(8)
b, Å	11.0827(4)
c, Å	17.6206(6)
β, deg	97.354(3)
V, $Å^3$	4199.6(3)
Z	4
ρ_{obs}, ρ_{cal}, g cm^{-3}	1.309(5), 1.304
F(000)	1712
μ, mm^{-1}	0.405
crystal size, mm	0.34 × 0.077 × 0.072
abs corn	analytical
radiation λ, Å	0.71073
temperature, K	100(2)
reflns collected, unique	10334, 3907 (R_{int} = 0.04)
limiting indices	$-26 \leq h \leq 26$, $-7 \leq k \leq 13$, $-21 \leq l \leq 19$
refinement method	full-matrix least squares on F^2
final *R* indices $[I > 2\sigma(I)]$[a]	R1 = 0.0351, wR2 = 0.0714
R indices (all data)[a]	R1 = 0.0513, wR2 = 0.0738
GOF on F^2	0.909
parameters/restraints	279/0

[a] $R1 = [(|F_o| - |F_c|)]/|F_o|$. $wR2 = [w|F_o|^2 - |F_c|^2)^2]/[w(|F_o|^2)^2]^{1/2}$.

■ RESULTS AND DISCUSSION

Synthesis of $([FeTPPbipy]^{\bullet})_n$. FeTPP-Cl (7 mg, 0.01 mmol), bipy (9.4 mg, 0.06 mmol), and 40 μL of NaOH (3M) were added to a mixture of DMF (3 mL) and ethanol (1 mL) in a small capped vial, sonicated to ensure homogeneity, and heated to 120 °C for 48 h, following by slow cooling to room temperature at 2 °C h^{-1}, yielding diffraction-quality dark-blue prismatic crystals. Anal. Calcd for $C_{54}H_{36}FeN_6$: C, 78.64; H, 4.39; N, 10.18%. Found: C, 78.45(8); H, 4.31(10); N, 9.86(6). ν_{max}/cm^{-1}: 3051, 3022, and 2964 [C(sp^2)H], 1600−1440 (CC), 1348 (CN), 1204 and 1070 (bipy), 1000 (FeTPP), 750 (CH) (Figure S2, Supporting Information).

Crystal Structure. The crystal structure of $([FeTPPbipy]^{\bullet})_n$ was determined by means of single-crystal X-ray diffraction. The structure consists of 1D coordination polymers extending along the [010] direction, where metalated porphyrins are axially bonded to two bipy ligands (Figure 1).

The resulting octahedral coordination sphere exhibits bond angles and distances that are typical for these types of compounds (Table 2).[37] These coordination polymers crystallize as shown in Figure 2. The connections between chains take place through *edge-to-face* π stacking along the [10−1] direction (centroid-to-centroid distance of 3.662 Å and angle of 83.94°). Additionally, there is a *face-to-face* π stacking along the [101] direction (centroid-to-centroid distance 5.067 Å and angle 0.02°). Therefore, the cohesion between 1D coordination polymers is based on a robust network of π bonds.

In principle, the chemical formula could be interpreted in terms of the presence of Fe^{II} and TPP^{2-} ions. However, as explained below, the behavior of $([FeTPPbipy]^{\bullet})_n$ is consistent with the presence of Fe^{III}. Therefore, because no further deprotonation is observed for the organic ligands, reduction of TPP^{2-} must be assumed to maintain neutrality.[38,39]

Distortion of the porphyrin was analyzed by the normal-coordinate structural decomposition method developed by Shelnutt et al.,[40,41] indicating a low saddle-type distortion (*sad*, B_{2u}). The contribution of this type of distortion (0.5967) to the total displacements is 67%, a, usual feature on low-spin iron(III) porphyrins.[42]

It is worth mentioning that, as far as we are aware, $([FeTPPbipy]^{\bullet})_n$ is the first Fe−TPP−dipyridyl coordination network exhibiting 1D polymers, and it has been formed by the assembly of neutral radical units. More details about the latter will be discussed below.

Purity of the Measured Samples. In order to determine the purity of the samples used for further characterization, the grinding effect on single crystals has been evaluated by means of X-ray diffraction. The results (Figure S3, Supporting Information) indicate that a significant rate of amorphization takes place. Taking this into consideration, magnetic susceptibility measurements and UV−visible spectroscopy were performed by using nonground single crystals introduced into a capillary in order to guarantee the purity of the sample. Unfortunately, the crystal features for $([FeTPPbipy]^{\bullet})_n$ were absolutely inadequate for the

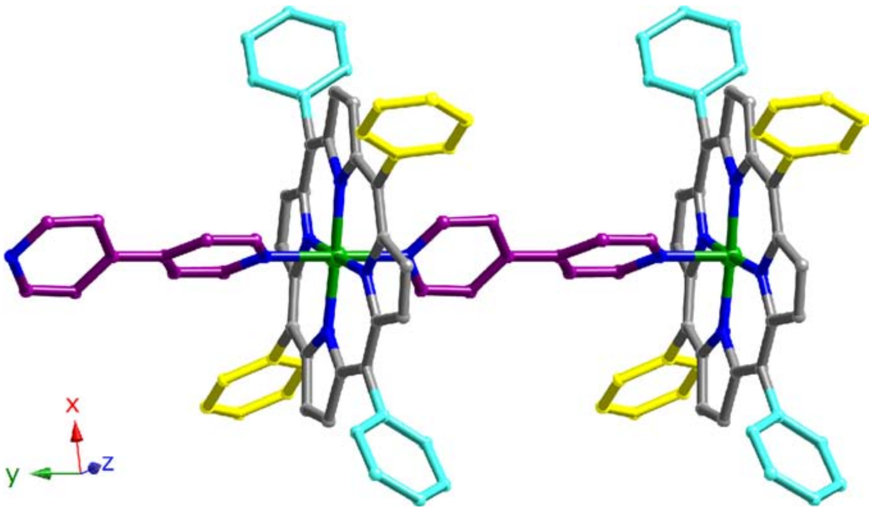

Figure 1. 1D coordination polymers extending along the [010] direction for $([\mathrm{FeTPPbipy}]^{\bullet})_n$. Color code: green, Fe; blue, N; gray, yellow, turquoise, C(porphyrin); purple, C(bipy). H atoms are omitted for clarity.

Table 2. Selected Bond Angles (deg) and Distances (Å) for $([\mathrm{FeTPPbipy}]^{\bullet})_n$ (Distances in Bold)[a]

			Octahedron $[\mathrm{FeN_6}]$			
Fe	N1	N1^{i}	N2	N2^{i}	N3	N4
N4	88.46(4)	88.46(4)	91.16(4)	91.16(4)	180	**1.998(2)**
N3	91.54(4)	91.54(4)	88.84(4)	88.84(4)	**1.985(2)**	
N2^{i}	90.14(6)	89.92(6)	177.69(8)	**1.996(1)**		
N2	89.92(6)	90.14(6)	**1.996(1)**			
N1^{i}	176.93(8)	**1.983(1)**				
N1	**1.983(1)**					

[a] Symmetry code: i, $-x$, y, $-z + {}^{1}/_{2}$.

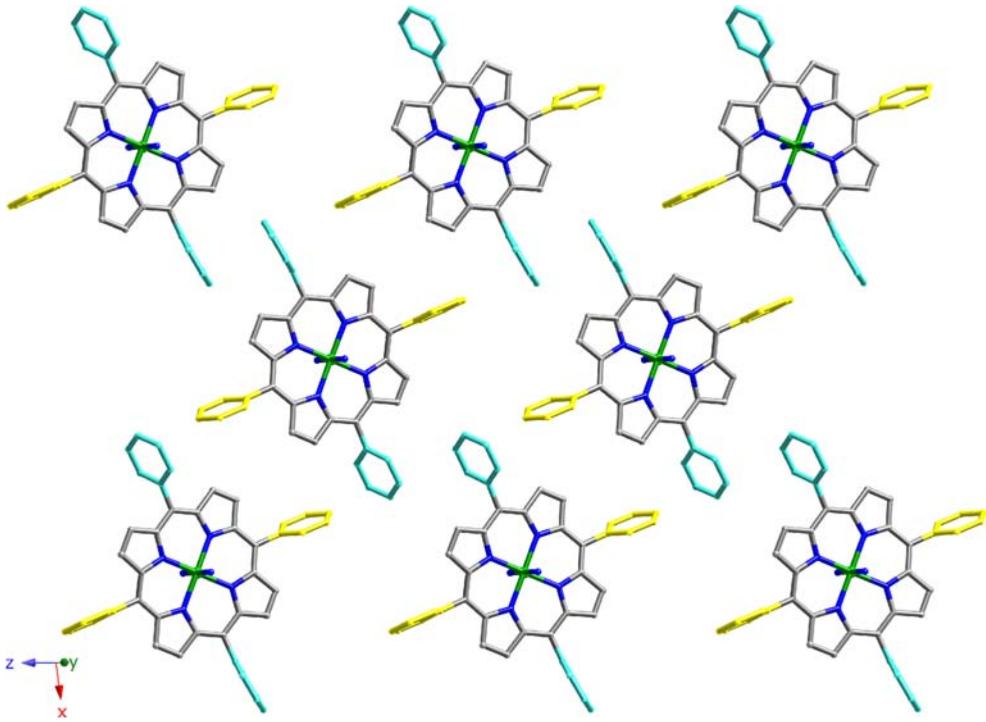

Figure 2. View of a (101) plane for $([\mathrm{FeTPPbipy}]^{\bullet})_n$. Color codes are the same as those in Figure 1. The bipy ligands and H atoms are omitted for clarity. *Face-to-face* π stacking occurs between the turquoise phenyl groups, and *edge-to-face* π stacking occurs between the turquoise and yellow phenyl groups.

performance of EPR and Mössbauer spectroscopies on single crystals.

UV−Visible (Diffuse-Reflectance) Spectroscopy. UV−visible spectroscopy was performed on nonground single

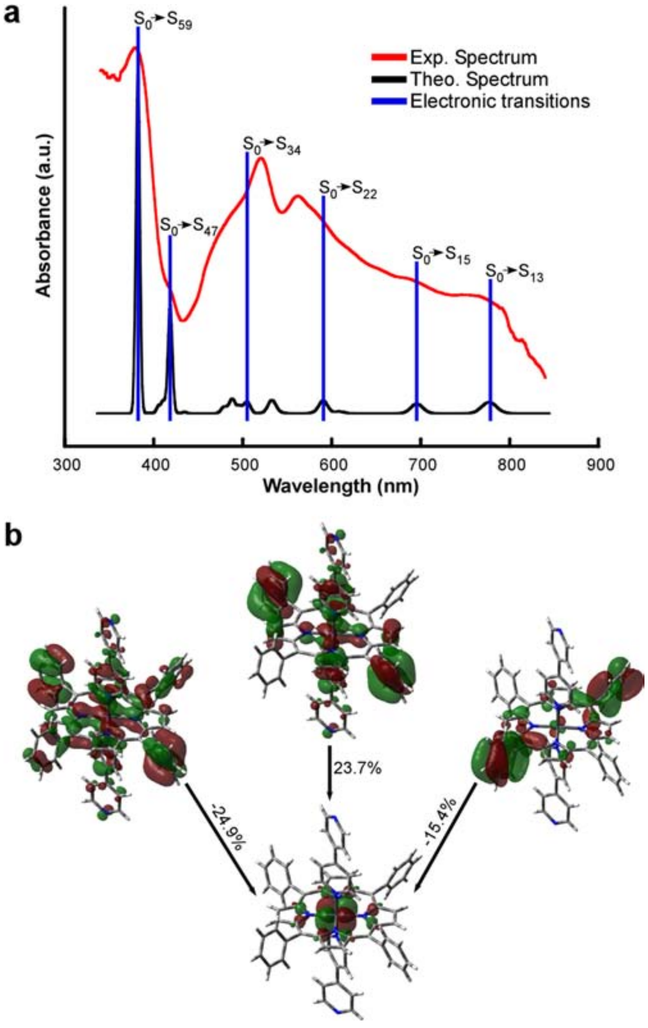

Figure 3. (a) Experimental and theoretical UV−visible spectra for ([FeTPPbipy]$^\bullet$)$_n$ and (b) molecular orbitals involved in the S_0−S_{59} transition.

crystals, and as observed in Figure 3a, the spectrum exhibits a Soret band (γ) at 377 nm and Q bands (β and α) at 517 and 557 nm, respectively. The fact that the Soret band is blue-shifted and reduced in intensity compared to typical six-coordinate low-spin ferric porphyrin complexes[25,43] is justified by assuming the presence of a radical species.[44,45] The low-spin iron(III) porphyrin characteristic L_1 and L_2 bands[46] appear at 815(sh) and 770 nm, respectively. A broad and weak band at 690 nm is in accordance with the presence of a porphyrinic radical.[44] These results were compared with the theoretical spectra (Figure 3a) obtained by TD-DFT calculations, performed by means of *Gaussian 03*[47] (B3LYP[48,49] functional and 6-31G valence). In addition to the good concordance between both spectra, the most remarkable fact is that the molecular orbitals involved in the Soret transition (S_0−S_{59}) represent an important charge transfer between the phenyl rings and the metal center (Figure 3b). This fact will be mentioned below during a discussion of the magnetic behavior.

EPR. X-band EPR spectroscopy was performed on ground single crystals of ([FeTPPbipy]$^\bullet$)$_n$. As observed, the spectrum shows two signals (Figure 4). The weakest of them (with g close to 6) is typical for magnetically isolated Fe^{III} systems in axial symmetry. Therefore, it is supposed to have been formed by crystal grinding. Unfortunately, the fact that grinding produces amorphization (Figure S3, Supporting Information) results in the impossibility of identifying this second phase by X-ray diffraction.

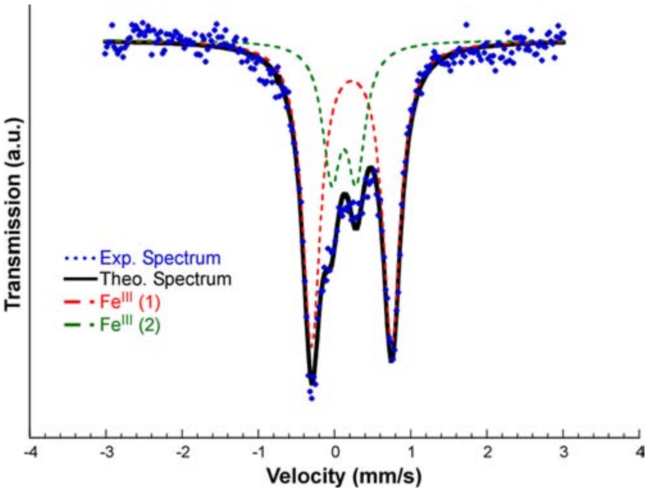

Figure 4. X-band EPR spectrum (room temperature) for ([FeTPPbipy]$^\bullet$)$_n$.

On the other hand, the principal signal (with g close to 2) can be interpreted in terms of the following two possibilities: (a) high-spin Fe^{III} ions in very low concentration in relation to the bulk of the analyzed sample and (b) low-spin Fe^{III} ions with either significant magnetic interactions between metal centers having different orientations or interactions with free radicals. In the latter case, radicals should be either delocalized or localized in such a way that they could relax in a short period of time. The first hypothesis does have a sense just for the case of high-spin Fe^{III} ions diluted in a low-spin Fe^{II} framework. This means that compound ([FeTPPbipy]$^\bullet$)$_n$ should contain Fe^{II} ions and that there are three contributions to the signal: the compound itself, the amorphous secondary phase, and a third unknown compound. This hypothesis has been discarded by X-band EPR spectroscopy at 100 K (Figure S4, Supporting Information) because it shows a broadening of the signal and a rapid decrease of the intensity (it mostly disappears below 50 K). This clearly indicates the presence of antiferromagnetic interactions, therefore pointing to the second explanation. Thus, the second explanation could just be feasible if the presence of free electrons is admitted because the structural characteristics of ([FeTPPbipy]$^\bullet$)$_n$ are not compatible with significant magnetic interactions between metal centers (the magnetic paths through the bipy ligands are too long). As explained below, these magnetic interactions were analyzed through measurements of the magnetic susceptibility and by DFT calculations.

Mössbauer Spectroscopy. Mössbauer spectroscopy was performed on ground single crystals. The spectrum has been simulated with the *NORMOS* program[50] and indicates the presence of two doublets: both of them corresponding to Fe^{III} signals. The presence of two Fe^{III} centers has been explained already in the EPR section, and it has been associated with amorphization of the sample as a consequence of the grinding, discarding the presence of a previous impurity.

The most significant signal is assigned to the metal ions in ([FeTPPbipy]$^\bullet$)$_n$, while the second one is assumed to be due to the secondary phase coming from grinding. Quantitative analysis reveals that the sample contained 70.5% by weight corresponding to ([FeTPPbipy]$^\bullet$)$_n$. This is in accordance with the significant rate of amorphization observed by X-ray diffraction (Figure S3, Supporting Information). Isomer shift (δ) and quadrupolar splitting (ΔE) values are 0.337(1) and 1.054(2) for the first signal and 0.235(2) and 0.326(7) for the second one, in the range usually observed for Fe^{III} ions (Figure 5).

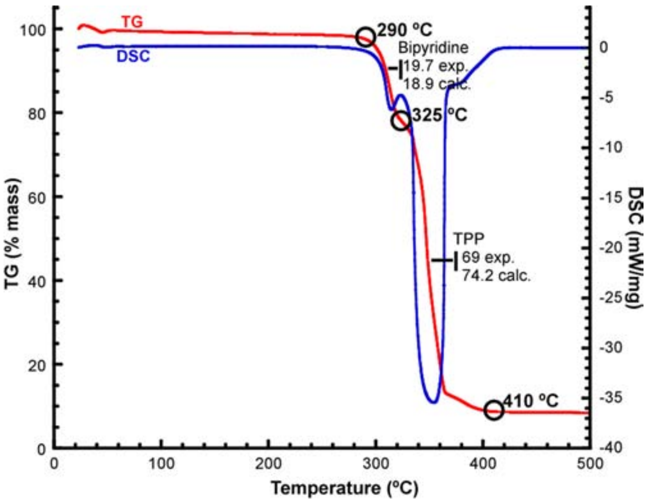

Figure 5. Mössbauer spectra for $([FeTPPbipy]^\bullet)_n$.

Thermogravimetry. Thermogravimetry analysis was carried out on nonground single crystals. The thermogravimetric decomposition curve of the compound shows an overlapped two-stage mass loss, from approximately 290 to 410 °C. As shown in Figure 6, the first step occurs between 290 and 325 °C with a 19.7% weight loss and the second step from 325 to 410 °C with a 69% weight loss. These mass percentages are close to the theoretical percentages of bipyridine (18.9%) and TPP (74.2%) molecules. The calcination product was identified by powder X-ray diffraction analysis, and it consists of Fe_2O_3 [space group $R\bar{3}c$, a = 5.0248 Å, c = 13.7163 Å, and γ = 120°].[51]

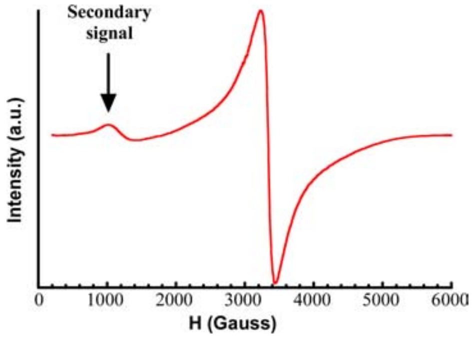

Figure 6. Thermal analysis for $([FeTPPbipy]^\bullet)_n$.

Magnetic Measurements. We have also performed magnetic susceptibility (χ_m) measurements for $([FeTPPbipy]^\bullet)_n$ in the range 4−300 K (Figure 7). It is worth mentioning that nonground single crystals were used for this analysis, but the original crystals were introduced into a capillary. The χ_mT value at room temperature is 0.30 cm^3 K mol^{-1}, which is much lower than the 4.37 cm^3 K mol^{-1} value expected for a high-spin Fe^{III} compound. On the contrary, it is close to the 0.37 cm^3 K mol^{-1} value expected for low-spin Fe^{III} complexes. As explained below (DFT calculations), the one-electron reduction of metalloporphyrin is analyzed, with the acquired electrons having been determined to be located on the phenyl groups. On the other hand, TD-DFT calculations carried out to analyze the UV−visible spectroscopy (Figure 3b) indicate that there is an important charge transfer between the phenyl rings and metal centers (Figure 3b). Thus, the slight discrepancy between the expected (0.30 cm^3 K mol^{-1}) and observed (0.37 cm^3 K mol^{-1}) χ_mT values for low-spin Fe^{III} can be explained if considering this charge transfer.

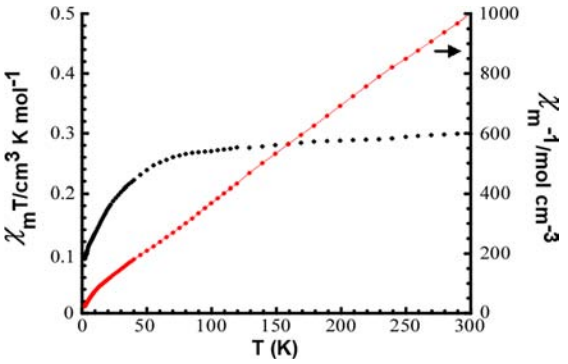

Figure 7. Thermal evolution of χ_mT and χ_m^{-1} for $([FeTPPbipy]^\bullet)_n$ and the corresponding theoretical Curie−Weiss law (red line).

The thermal evolution of the reciprocal susceptibility follows the Curie−Weiss law with C_m = 0.32 cm^3 K mol^{-1} and θ = −18.7 K (Figure 7). The product χ_mT continuously decreases upon cooling, reaching a value of 0.09 cm^3 K mol^{-1} at 5.0 K, indicating the presence of antiferromagnetic interactions, as expected from EPR characterization. As mentioned, these interactions cannot be attributed to magnetic exchange between metal centers. Therefore, coupling between metal ions and free electrons should be admitted.

DFT Calculations. As previously mentioned, the structural characterization of this compound could make one think that the metal ion is Fe^{II}, in accordance with the presence of TPP^{2-} ligands and neutral bipy molecules. However, the commercial reactant, [FeTPPCl], contains Fe^{III}, and its reduction to Fe^{II} does not seem to be feasible. On the other hand, the bond distances and angles are typical for iron(III) porphyrins, and the rest of the characterization techniques clearly indicate that the metal ion is Fe^{III}. Therefore, the best of our hypothesis is that the compound has been formed by the assembly of $[FeTPP]^\bullet$ radical structural units, which extend, producing 1D polymers by means of the axial coordination of the metal center to bipy ligands. Thus, the $[FeTPP]^\bullet$ structural units should be thought of as being the result of one-electron reduction of the metalloporphyrin (reactions 1 and 2).

$$[FeTPPC1] \rightarrow [FeTPP]^+ + Cl^- \qquad (1)$$

$$[FeTPP]^+ + e^- \rightarrow [FeTPP]^\bullet \qquad (2)$$

Admitting that reduction must have taken place for the metalloporphyrin, we tried to identify the reductant agent. Even if there are some calculated redox potentials in the literature,[52] they are not useful in our case because of the nonstandard conditions for solvothermal synthesis. Even so, there are several possible reductant agents like residues of bipy and DMF.[53]

Thus, next question about $([FeTPPbipy]^\bullet)_n$ consists of determining the localization of the electron providing the metalloporphyrins with its radical nature. In the case of $([FeTPPbipy]^\bullet)_n$, the presence of low-spin Fe^{III} and an extra unpaired electron should result in two unpaired electrons per metalloporphyrin. Therefore, we could think of two explanations. As previously proposed,[54] the extra unpaired electron could be delocalized on the aromatic

Scheme 1. Possibilities for the Number of Unpaired Electrons Depending on the Occurrence of Antiferromagnetic Coupling through π Stacking

Possible interactions between 1D polymers per two Fe^{III} centers

	1D polymer 1		**1D polymer 2**		**π-stacking producing antiferromagnetic interactions**
	Fe	TPP	TPP	Fe	
4 unpaired electrons per two Fe^{III} centers	↑	↑	↑	↑	No
2 unpaired electrons per two Fe^{III} centers	↓	↑↓		↑	Yes

porphyrinic system. If analysis of the compound is done from the point of view of isolated structural units (1D polymers), this could be an effective explanation. However, magnetic measurements are not consistent with the latter. Besides, there is an intricate π-stacking system in $([\mathrm{FeTPPbipy}]^{\bullet})_n$ according to which analysis of the framework from such a point of view does not seem to be adequate. Thus, a second explanation is that the electrons acquired by reduction are paired in the 3D framework (Scheme 1). This idea is strongly supported by π stacking because it provides the opportunity of electron coupling.

In order to provide theoretical support to the abovementioned aspects, both hypotheses were analyzed by means of quantum-mechanical DFT calculations (*Gaussian 03* program).[47] Calculations were performed using Becke's three-parameter hybrid functional with the correlation functional of Lee, Yang, and Parr (B3LYP)[48,49] with a split-valence basis set of 6-31G. This functional does not consider the dispersive interactions. However, it has been selected because our objective was not obtaining an accurate value for the energy but representative values for a comparison between both hypotheses. In fact, the goal was to investigate the effect of π stacking on the stability of the framework. To this purpose, two dimeric fragments $(\mathrm{FeTPPbipy_2})_2$ were selected. In dimer 1, the interdimer connection is due to the *edge-to-face* π bond along the [10−1] direction, while in dimer 2, the connection takes place by the *face-to-face* π bond along the [101] direction (Figure 8a). For each dimer, two calculations (Table 3) were carried out: in calculation 1, the dimer has four unpaired electrons (two per monomer), and in calculation 2, the dimer has two unpaired electrons (one per monomer). Therefore, calculation 1 accounts for the first hypothesis (that is, analysis from the point of view of isolated 1D polymers), while calculation 2 explores the possibility of electron coupling through interpolymer π stacking. Obviously, extension of the framework through the three directions of space should have been considered for more accurate calculations. However, the large amount of atoms involved makes this very expensive.

Table 3 summarizes the as-calculated values. As observed, the values show that for both dimers the situation with one unpaired electron per monomer (two per dimer) is more stable than the situation with two unpaired electrons per monomer (four per dimer), supporting the idea that π stacking is responsible for stabilization of the framework.

At this point of the discussion, claiming that π stacking is responsible for stabilization of the framework seems to be obvious. Nevertheless, the remarkable point is that calculations strongly support the idea that the extra electrons have not been delocalized on the TPP pyrrolic system but they are paired in molecular orbitals formed by π stacking. In fact, as observed in Figure 8b,c, the calculations provided molecular orbitals for these interactions.

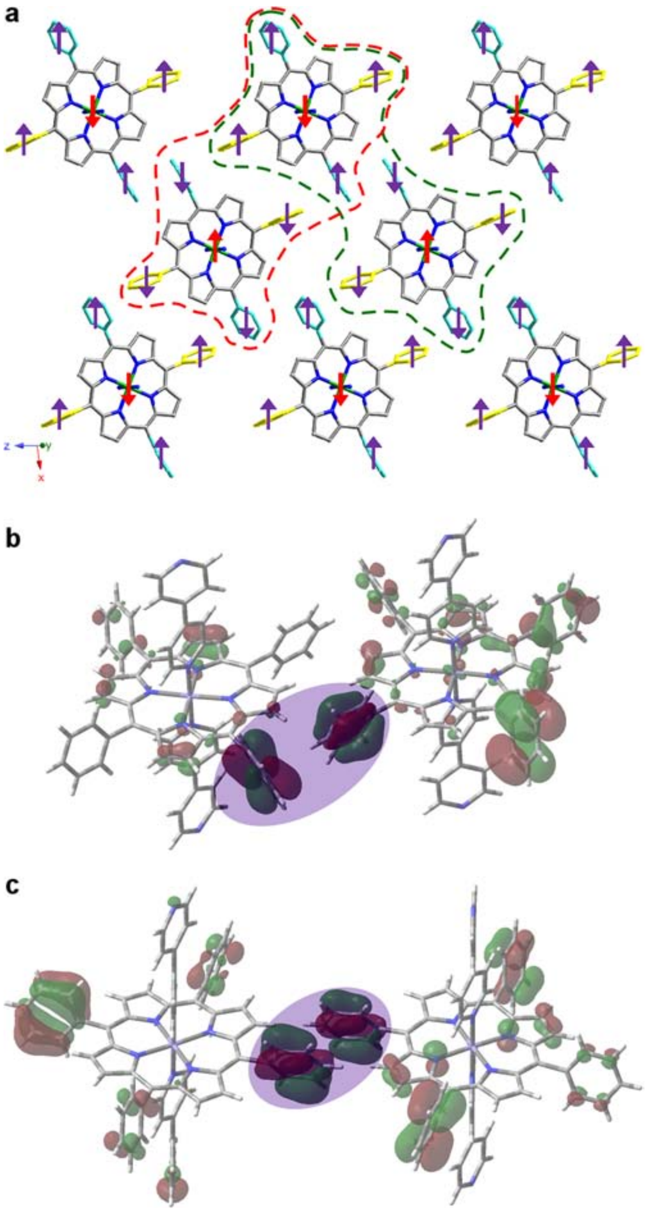

Figure 8. (a) Selected dimeric fragments for the DFT calculations according to *edge-to-face* (red line) and *face-to-face* (green line) π interactions. A scheme for the spin distribution proposal is also shown: red arrows are the unpaired electrons corresponding to low-spin Fe^{III} (d^5), and each group of four purple arrows corresponds to a single electron localized on the phenyl groups belonging to the same metalloporphyrin. (b) Calculated molecular orbitals involving the *edge-to face* and (c) *face-to-face* π stackings.

Table 3. Calculated Energy for $(FeTPPbipy_2)_2$ Dimers

dimer	π interactions	coupling through π interactions	no. of unpaired electrons per dimer	calculated energy (hartree)
1	*edge-to-face*	yes	2	−8331.1805358
1	*edge-to-face*	no	4	−8331.1309928
2	*face-to-face*	yes	2	−8331.1814716
2	*face-to-face*	no	4	−8331.1533709

Self-Assembly of Neutral Radicals. As π stacking is extended on the (101) planes, extrapolation of the DFT calculations to the 3D network can be done. As observed in Figure 8b,c, the contribution of the phenyl molecular orbitals to π stacking is consistent with this extrapolation. First of all, the electron acquired by the porphyrin could be thought of as delocalized on the four phenyl groups. On the other hand, if considering that magnetic measurements are consistent with the presence of a value close to one unpaired electron per monomer, the spin distribution proposed in Figure 8a could be a reasonable explanation for the behavior of this compound. This spin distribution is based on the occurrence of antiferromagnetic coupling not only between electrons belonging to the metal center and phenyl groups (as previously mentioned in the Magnetic Measurements section) but also between phenyl electrons localized on adjacent 1D polymers, as seen in Figure 8b,c.

In summary, identification of the localization of the acquired electrons is the key point that supports the idea of neutral radicals having been able to self-assemble, producing such a 3D framework.

CONCLUSIONS

The compound $([FeTPPbipy]^{\bullet})_n$ has been formed by the assembly of metalloporphyrinic neutral radicals that have been formed by one-electron reduction of the original $[FeTPP]^+$ cations, as suggested by the presence of low-spin Fe^{III} ions. The as-acquired electrons are proposed to be paired in the molecular orbitals formed by π−π interactions between the phenyl groups of different 1D polymers. The resulting packing is the first Fe−TPP−bipy coordination network exhibiting 1D polymers.

ASSOCIATED CONTENT

Supporting Information

ORTEP detail of the structure, IR and EPR spectra, X-ray measurements, crystallographic data, and a CIF file for CCDC 888109. This material is available free of charge via the Internet at http://pubs.acs.org.

AUTHOR INFORMATION

Corresponding Author

*E-mail: gotzone.barandika@ehu.es.

Author Contributions

The manuscript was written through contributions of all authors. All authors have given approval to the final version of the manuscript. All authors contributed equally.

Notes

The authors declare no competing financial interest.

ACKNOWLEDGMENTS

This work has been financially supported by the "Ministerio de Ciencia e Innovación" (MAT2010-15375), the "Gobierno Vasco" (Basque University System Research Groups, IT-630-13), and UPV/EHU (UFI 11/15), which we gratefully acknowledge. SGIker (UPV/EHU) technical support (MEC, GV/EJ, European Social Fund) is gratefully acknowledged. The authors thank Dr. Fernando Plazaola (UPV/EHU) for her help in interpreting the Mössbauer spectra. A.F.-M. thanks the UPV/EHU for fellowships.

REFERENCES

(1) Beletskaya, I.; Tyurin, V. S.; Tsivadze, A. Y.; Guilard, R.; Stern, C. *Chem. Rev.* **2009**, *109*, 1659−1713.

(2) Drain, C. M.; Varotto, A.; Radivojevic, I. *Chem. Rev.* **2009**, *109*, 1630−1658.

(3) Wang, C.; Xie, Z.; deKrafft, K. E.; Lin, W. *J. Am. Chem. Soc.* **2011**, *133*, 13445−13454.

(4) Margelefsky, E. L.; Zeidan, R. K.; Davis, M. E. *Chem. Soc. Rev.* **2008**, *37*, 1118−1126.

(5) Mola, J.; Mas-Marza, E.; Sala, X.; Romero, I.; Rodriguez, M.; Vinas, C.; Parella, T.; Llobet, A. *Angew. Chem., Int. Ed.* **2008**, *47*, 5830−5832.

(6) Zou, C.; Wu, C.-D. *Dalton Trans.* **2012**, *41*, 3879−3888.

(7) Shultz, A. M.; Farha, O. K.; Hupp, J. T.; Nguyen, S. T. *J. Am. Chem. Soc.* **2009**, *131*, 4204−4205.

(8) Gao, B.; Zhao, J.; Li, Y. *J. Appl. Polym. Sci.* **2011**, *122*, 406−416.

(9) Mohnani, S.; Bonifazi, D. *Coord. Chem. Rev.* **2010**, *254*, 2342−2362.

(10) Zeitouny, J.; Aurisicchio, C.; Bonifazi, D.; De Zorzi, R.; Geremia, S.; Bonini, M.; Palma, C.-A.; Samori, P.; Listorti, A.; Belbakra, A.; Armaroli, N. *J. Mater. Chem.* **2009**, *19*, 4715−4724.

(11) Liu, C.-X.; Liu, Q.; Guo, C.-C.; Tan, Z. *J. Porphyrins Phthalocyanines* **2010**, *14*, 825−831.

(12) Castro, K. A. D. F.; Halma, M.; Machado, G. S.; Ricci, G. P.; Ucoski, G. M.; Ciuffi, K. J.; Nakagaki, S. *J. Braz. Chem. Soc.* **2010**, *21*, 1329−1340.

(13) Serwicka, E. M.; Poltowicz, J.; Bahranowski, K.; Olejniczak, Z.; Jones, W. *Appl. Catal., A* **2004**, *275*, 9−14.

(14) Schuenemann, V.; Trautwein, A. X.; Rietjens, I. M. C. M.; Boersma, M. G.; Veeger, C.; Mandon, D.; Weiss, R.; Bahl, K.; Colapietro, C.; Piech, M.; Austin, R. N. *Inorg. Chem.* **1999**, *38*, 4901−4905.

(15) Cooke, P. R.; Gilmartin, C.; Gray, G. W.; Lindsay Smith, J. R. *J. Chem. Soc., Perkin Trans. 2* **1995**, *2*, 1573−1578.

(16) Hilal, H. S.; Kim, C.; Sito, M. L.; Schreiner, A. F. *J. Mol. Catal.* **1991**, *64*, 133−142.

(17) Garibay, S. J.; Stork, J. R.; Cohen, S. M. *Prog. Inorg. Chem.* **2009**, *56*, 335−378.

(18) Burnett, B. J.; Barron, P. M.; Choe, W. *CrystEngComm* **2012**, *14*, 3839−3846.

(19) Kumar, R. K.; Balasubramanian, S.; Goldberg, I. *Chem. Commun.* **1998**, 1435−1436.

(20) Tsao, T.-B.; Lee, G.-H.; Yeh, C.-Y.; Peng, S.-M. *Dalton Trans.* **2003**, 1465−1471.

(21) Kumar, D. K.; Das, A.; Dastidar, P. *Inorg. Chem.* **2007**, *46*, 7351−7361.

(22) Diskin-Posner, Y.; Patra, G. K.; Goldberg, I. *J. Chem. Soc., Dalton Trans.* **2001**, 2775−2782.

(23) Wang, Q.-G.; Xie, Y.-S.; Zeng, F.-H.; Ng, S.-W.; Zhu, W.-H. *Inorg. Chem. Commun.* **2010**, *13*, 929−931.

(24) Burrell, A. K.; Officer, D. L.; Reid, D. C. W.; Wild, K. Y. *Angew. Chem., Int. Ed.* **1998**, *37*, 114−117.

(25) Mikami, S.; Sugiura, K.-i.; Maruta, T.; Maeda, Y.; Ohba, M.; Usuki, N.; Okawa, H.; Akutagawa, T.; Nisihara, S.; Nakamura, T.; Iwasaki, K.; Miyazaki, N.; Hino, S.; Asato, E.; Miller, J. S.; Sakata, Y. *J. Chem. Soc., Dalton Trans.* **2001**, 448−455.

(26) Summerville, D. A.; Cohen, I. A.; Hatano, K.; Scheidt, W. R. *Inorg. Chem.* **1978**, *17*, 2906−2910.

(27) Calderon-Casado, A.; Barandika, G.; Bazan, B.; Urtiaga, M.-K.; Vallcorba, O.; Rius, J.; Miravittles, C.; Arriortua, M.-I. *CrystEngComm* **2011**, *13*, 6831−6838.

(28) Barandika, M. G.; Hernandez-Pino, M. L.; Urtiaga, M. K.; Cortes, R.; Lezama, L.; Arriortua, M. I.; Rojo, T. *J. Chem. Soc., Dalton Trans.* **2000**, 1469−1473.

(29) Barandika, M. G.; Cortes, R.; Serna, Z.; Lezama, L.; Rojo, T.; Urtiaga, M. K.; Arriortua, M. I. *Chem. Commun.* **2001**, 45−46.
(30) de la Pinta, N.; Martin, S.; Urtiaga, M. K.; Barandika, M. G.; Arriortua, M. I.; Lezama, L.; Madariaga, G.; Cortes, R. *Inorg. Chem.* **2010**, *49*, 10445−10454.
(31) Hernandez, M. L.; Urtiaga, M. K.; Barandika, M. G.; Cortes, R.; Lezama, L.; de la Pinta, N.; Arriortua, M. I.; Rojo, T. *J. Chem. Soc., Dalton Trans.* **2001**, 3010−3014.
(32) Serna, Z. F.; Lezama, L.; Urtiaga, M. K.; Arriortua, M. I.; Barandika, M. G.; Cortes, R.; Rojo, T. *Angew. Chem., Int. Ed.* **2000**, *39*, 344−347.
(33) Fidalgo-Marijuan, A.; Barandika, G.; Bazan, B.; Urtiaga, M.-K.; Arriortua, M.-I. *Polyhedron* **2011**, *30*, 2711−2716.
(34) DeVries, L. D.; Choe, W. *J. Chem. Crystallogr.* **2009**, *39*, 229−240.
(35) Yinghua, W. *J. Appl. Crystallogr.* **1987**, *20*, 258−259.
(36) Sheldrick, G. M. *Acta Crystallogr., Sect. A: Found. Crystallogr.* **2008**, *A64*, 112−122.
(37) Scheidt, W. R.; Geiger, D. K.; Haller, K. J. *J. Am. Chem. Soc.* **1982**, *104*, 495−499.
(38) Saffari, J.; Khorasani-Motlagh, M.; Noroozifar, M. *Synth. React. Inorg., Met.−Org., Nano-Met. Chem.* **2010**, *40*, 899−904.
(39) Mezger, M.; Hanack, M.; Hirsch, A.; Kleinwaechter, J.; Mangold, K. M.; Subramanian, L. R. *Chem. Ber.* **1991**, *124*, 841−847.
(40) Jentzen, W.; Song, X.-Z.; Shelnutt, J. A. *J. Phys. Chem. B* **1997**, *101*, 1684−1699.
(41) Jentzen, W.; Ma, J.-G.; Shelnutt, J. A. *Biophys. J.* **1998**, *74*, 753−763.
(42) Ohgo, Y.; Hoshino, A.; Okamura, T.; Uekusa, H.; Hashizume, D.; Ikezaki, A.; Nakamura, M. *Inorg. Chem.* **2007**, *46*, 8193−8207.
(43) Quinn, R.; Strouse, C. E.; Valentine, J. S. *Inorg. Chem.* **1983**, *22*, 3934−3940.
(44) Ikezaki, A.; Tukada, H.; Nakamura, M. *Chem. Commun.* **2008**, 2257−2259.
(45) Gans, P.; Buisson, G.; Duee, E.; Marchon, J. C.; Erler, B. S.; Scholz, W. F.; Reed, C. A. *J. Am. Chem. Soc.* **1986**, *108*, 1223−1234.
(46) Ochiai, E.-i. *Bioinorganic Chemistry: An Introduction*; Allyn and Bacon, Inc.: Boston, MA, 1977; Chapter 5.
(47) Frisch, M. J.; Trucks, G. W.; Schlegel, H. B.; Scuseria, G. E.; Robb, M. A.; Cheeseman, J. R.; Montgomery, J. A., Jr.; Vreven, T.; Kudin, K. N.; Burant, J. C.; Millam, J. M.; Iyengar, S. S.; Tomasi, J.; Barone, V.; Mennucci, B.; Cossi, M.; Scalmani, G.; Rega, N.; Petersson, G. A.; Nakatsuji, H.; Hada, M.; Ehara, M.; Toyota, K.; Fukuda, R.; Hasegawa, J.; Ishida, M.; Nakajima, T.; Honda, Y.; Kitao, O.; Nakai, H.; Klene, M.; Li, X.; Knox, J. E.; Hratchian, H. P.; Cross, J. B.; Bakken, V.; Adamo, C.; Jaramillo, J.; Gomperts, R.; Stratmann, R. E.; Yazyev, O.; Austin, A. J.; Cammi, R.; Pomelli, C.; Ochterski, J. W.; Ayala, P. Y.; Morokuma, K.; Voth, G. A.; Salvador, P.; Dannenberg, J. J.; Zakrzewski, V. G.; Dapprich, S.; Daniels, A. D.; Strain, M. C.; Farkas, O.; Malick, D. K.; Rabuck, A. D.; Raghavachari, K.; Foresman, J. B.; Ortiz, J. V.; Cui, Q.; Baboul, A. G.; Clifford, S.; Cioslowski, J.; Stefanov, B. B.; Liu, G.; Liashenko, A.; Piskorz, P.; Komaromi, I.; Martin, R. L.; Fox, D. J.; Keith, T.; Al-Laham, M. A.; Peng, C. Y.; Nanayakkara, A.; Challacombe, M.; Gill, P. M. W.; Johnson, B.; Chen, W.; Wong, M. W.; Gonzalez, C.; Pople, J. A. *Gaussian 03*, revision D.02; Gaussian, Inc.: Wallingford, CT, 2004.
(48) Becke, A. D. *J. Chem. Phys.* **1993**, *98*, 5648−5652.
(49) Lee, C.; Yang, W.; Parr, R. G. *Phys. Rev. B: Condens. Matter* **1988**, *37*, 785−789.
(50) Brand, R. A.; Lauer, J.; Herlach, D. M. *J. Phys. F: Met. Phys.* **1983**, *13*, 675−683.
(51) Tsirel'son, V. G.; Antipin, M. Y.; Strel'tsov, V. A.; Ozerov, R. P.; Struchkov, Y. T. *Dokl. Akad. Nauk SSSR* **1988**, *298*, 1137−1141.
(52) Ou, Z.; E, W.; Zhu, W.; Thordarson, P.; Sintic, P. J.; Crossley, M. J.; Kadish, K. M. *Inorg. Chem.* **2007**, *46*, 10840−10849.
(53) Pereira, M. M.; Abreu, A. R.; Goncalves, N. P. F.; Calvete, M. J. F.; Simoes, A. V. C.; Monteiro, C. J. P.; Arnaut, L. G.; Eusebio, M. E.; Canotilho, J. *Green Chem.* **2012**, *14*, 1666−1672.
(54) Scheidt, W. R.; Brancato-Buentello, K. E.; Song, H.; Reddy, K. V.; Cheng, B. *Inorg. Chem.* **1996**, *35*, 7500−7507.